Available online at www.sciencedirect.com

SciVerse ScienceDirect

Ceramics International 39 (2013) 5967–5971

CERAMICS INTERNATIONAL

www.elsevier.com/locate/ceramint

Short communication

Crystal structure and dielectric behavior of pseudo-cubic perovskite oxides

Young-Il Kim[a,*], Young-Hun Kim[b], Jong-Sook Lee[b]

[a]Department of Chemistry, Yeungnam University, Gyeongsan 712-749, Republic of Korea
[b]School of Materials Science and Engineering, Chonnam National University, Gwangju 500-757, Republic of Korea

Received 21 November 2012; received in revised form 14 December 2012; accepted 15 December 2012
Available online 25 December 2012

Abstract

Complex perovskites $(BaM_{0.9}M'_{0.1})_{0.984}O_3$ (M = Ti, Zr; M′ = Nb, Ta) were prepared by a solid-state reaction at 1300 − 1600 °C. High-resolution synchrotron X-ray powder diffraction confirmed that all samples, except for MM′ = ZrNb, could form a solid solution single phase. All four samples appear to have empty *d* bands with optical band gaps wider than 3.2 eV. This suggests that the defects generated by the aliovalent substitutions of M^{4+}/M'^{5+} were compensated by cation vacancies, not by reduction of the transition metal. In contrast to tetragonal and polar $BaTiO_3$, its derivatives $(BaTi_{0.9}M'_{0.1})_{0.984}O_3$ (M′ = Nb, Ta) were stabilized in a simple cubic average structure (space group $Pm\bar{3}\ m$) at room temperature. Such structural and compositional modifications of $BaTiO_3$ led to marked evolution of the dielectric behavior: suppression of the temperature-dependent phase transitions and an increase in the dielectric constant. On the other hand, $(BaZr_{0.9}Ta_{0.1})_{0.984}O_3$ remained isostructural to $BaZrO_3$ and the dielectric properties remained relatively unchanged.

Keywords: C. Electrical properties; D. Perovskites; D. $BaTiO_3$ and titanates

1. Introduction

Perovskite oxides with d^0 transition metals (Ti^{4+}, Zr^{4+}, Nb^{5+}, Ta^{5+}, etc.) have attracted considerable attention owing to their diverse functions as semiconductors, dielectrics, piezoelectrics, ionic conductors and catalysts [1,2]. Barium titanate ($BaTiO_3$), in both undoped stoichiometric and doped non-stoichiometric forms, is one of the most studied perovskite materials owing its unique properties, such as ferroelectricity and phase transitions [3]. A range of doping strategies have been adopted to tailor the crystal structure and electrical/optical properties of $BaTiO_3$. On the other hand, barium zirconate ($BaZrO_3$) has attracted attention as a paraelectric insulator with excellent thermal (melting point ≈ 2700 °C) and chemical stability, as well as a small temperature coefficient of the dielectric constant [4].

This study compared the crystal structures and dielectric properties of $(BaM_{0.9}M'_{0.1})_{0.984}O_3$ with those of $BaMO_3$. In particular, aliovalent substitutions in $BaMO_3$ (M = Ti, Zr) using group 5B metals (M′ = Nb, Ta) as substituents were investigated. In contrast to conventional M^{4+}/M'^{5+} substitutions in $BaMO_3$ [5], the compositional ratio was set to Ba:(M + M′) = 1:1, so that vacancies can be generated on both the octahedral and dodecahedral sites of the perovskite lattice. The substitution level was fixed to 10%. As the perovskite lattice does not allow interstitial oxygen, the substitution products can be represented as $(BaM_{0.9}M'_{0.1})_{0.984}O_3$ rather than $BaM_{0.9}M'_{0.1}O_{3.05}$. From a comparison of the six-coordinate ionic radii of Ti^{4+} (0.605 Å), Zr^{4+} (0.72 Å), Nb^{5+} (0.64 Å) and Ta^{5+} (0.64 Å) [6], it is expected that the partial substitution of Nb (or Ta) for Ti (or Zr) should introduce substantial local geometric distortion in the lattices of tetragonal $BaTiO_3$ or cubic $BaZrO_3$, which should affect the dielectric behavior.

2. Experimental

2.1. Sample preparation

Simple perovskites, $BaMO_3$ (M = Ti, Zr), and quaternary complex ones, $(BaM_{0.9}M'_{0.1})_{0.984}O_3$ (M′ = Nb, Ta),

*Corresponding author. Tel.: +82 53 810 2353; fax: +82 53 810 4613.
E-mail addresses: yikim@ynu.ac.kr, eternalday@gmail.com (Y.-I. Kim).

0272-8842/$ - see front matter © 2012 Elsevier Ltd and Techna Group S.r.l. All rights reserved.
http://dx.doi.org/10.1016/j.ceramint.2012.12.053

Table 1
Nominal composition and heating conditions of the samples.

Sample	Cation composition	Final heating
BTO	Ba:Ti=1:1	1300 °C, 12 h
BTNO	Ba:Ti:Nb=1:0.9:0.1	1350 °C, 12 h
BTTO	Ba:Ti:Ta=1:0.9:0.1	1350 °C, 12 h
BZO	Ba:Zr=1:1	1550 °C, 12 h
BZNO	Ba:Zr:Nb=1:0.9:0.1	1600 °C, 12 h
BZTO	Ba:Zr:Ta=1:0.9:0.1	1550 °C, 12 h

were prepared in polycrystalline form using a high-temperature solid-state process with $BaCO_3$ (Alfa, 99.95%), TiO_2 (Aldrich, 99.99%), ZrO_2 (Aldrich, 99%), Nb_2O_5 (Alfa, 99.9985%) and Ta_2O_5 (Alfa, 99.85%) as the starting materials. The powder reagents were mixed at the required quantitative ratio of metal components, and heated to 900 °C for 12 h. The calcined powder was pressed into pellets and heated to a designated temperature point between 1200 and 1600 °C for 6 h. The heating procedure was repeated 4–8 times, increasing the dwell temperature stepwise, until there was no improvement in the phase purity. Table 1 lists the abbreviated sample notations and corresponding preparation conditions.

2.2. Characterizations

X-ray powder diffraction (XPD) was used to monitor the reaction progress and determine the crystal structure of the products. High-resolution synchrotron XPD was performed at Beamline 8C2 of the Pohang Accelerator Laboratory, Korea, which provided parallel beam radiation of $\lambda = 1.550$ Å. The data was recorded in reflection mode at room temperature over the 2θ range, $10-130^\circ$, at 0.01° 2θ steps per 3 s. For crystal structure refinement, Rietveld analysis was performed using the GSAS-GUI software suite [7,8]. The microstructure of the fractured surface of the pellet samples was observed by field-emission scanning electron microscopy (FE-SEM; S-4700, Hitachi).

Diffuse-reflectance absorbance spectroscopy was conducted in a double-beam spectrometer (Neosys-2000, Scinco) equipped with a 35 mm integrating sphere. The reflectance (R) was measured over the wavelength range, 200 – 800 nm (6.20 – 1.55 eV), using $BaSO_4$ as the reference standard. The measured R value was converted to a Kubelka–Munk function [9] from which the band gap energy (E_g) was estimated [10].

The dielectric properties were measured using a LCR meter (HP4284A) for the frequency range, from 20 Hz to 1 MHz, where pellet specimens with $\approx 20\%$ porosity were used. The samples were loaded in a closed cycle refrigerator (CCR) with a high-temperature option (CCS-400/202, Janis, USA) at temperatures ranging from −223 °C to 227 °C.

3. Results and discussion

Fig. 1 compares the XPD patterns of all six samples listed in Table 1. The simple perovskites BTO and BZO presented the patterns that correspond well to the respective room temperature crystal structures [3,4]. Solid solutions, BTNO, BTTO and BZTO, were obtained as a single phase by heat treatment at 1350 °C (M = Ti) or 1550 °C (M = Zr). In each case, $Ba_5M'_4O_{15}$ (M′ = Nb or Ta) appeared as an intermediate phase at lower heating temperatures. On the other hand, BZNO did not reach a single phase according to XPD but was fractionated into two cubic phases with different cell parameters.

Both BTNO and BTTO had cubic symmetry on average, in contrast to the parental BTO. It is well known that $BaTiO_3$ has an oversized octahedral cavity for Ti^{4+}, which eventually leads to tetragonal distortion and an acentric crystal lattice at room temperature. Above result shows that the incorporation of larger substituents, Nb^{5+} or Ta^{5+}, into $BaTiO_3$ stabilizes the cubic structure at room temperature. The cell parameters were determined from Rietveld refinements over the 2θ range, $10-130^\circ$, and are listed in Table 2. The lattice volumes of BTNO and BTTO were larger than those of BTO, which is in accordance with the relative sizes of Ti^{4+} and substituent ions.

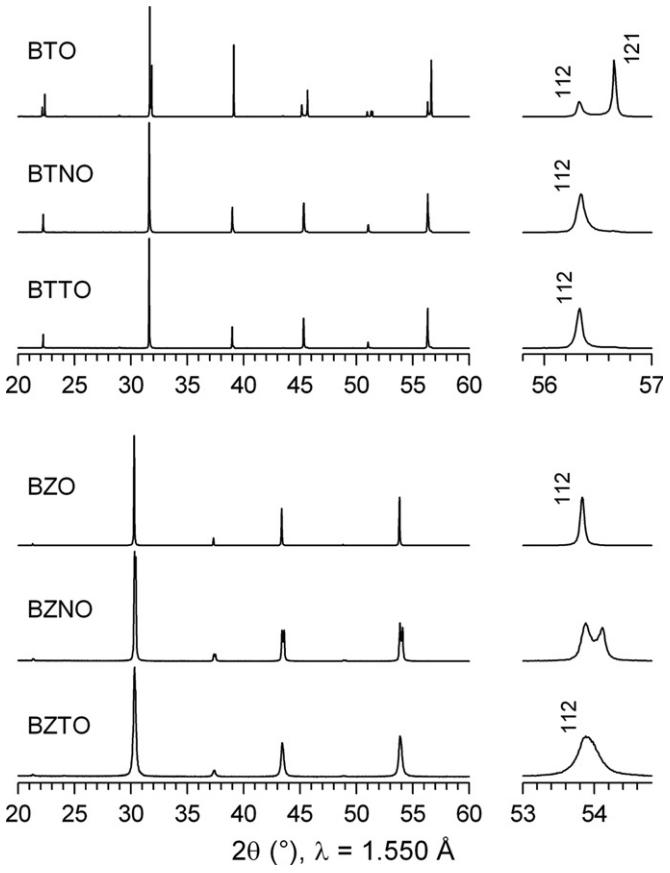

Fig. 1. XPD patterns of the titanate (BTO, BTNO, BTTO) and zirconate (BZO, BZNO, BZTO) samples.

Table 2
Space groups and cell parameters from the Rietveld refinement.

Sample	Space group	a (Å)	c (Å)	V (Å^3)
BTO	$P4mm$	3.99410(1)	4.03598(2)	64.385(1)
BTNO	$Pm\bar{3}m$	4.02126(2)		65.026(1)
BTTO	$Pm\bar{3}m$	4.02224(1)		65.074(1)
BZO	$Pm\bar{3}m$	4.19368(1)		73.754(1)
BZTO	$Pm\bar{3}m$	4.18778(4)		73.443(2)

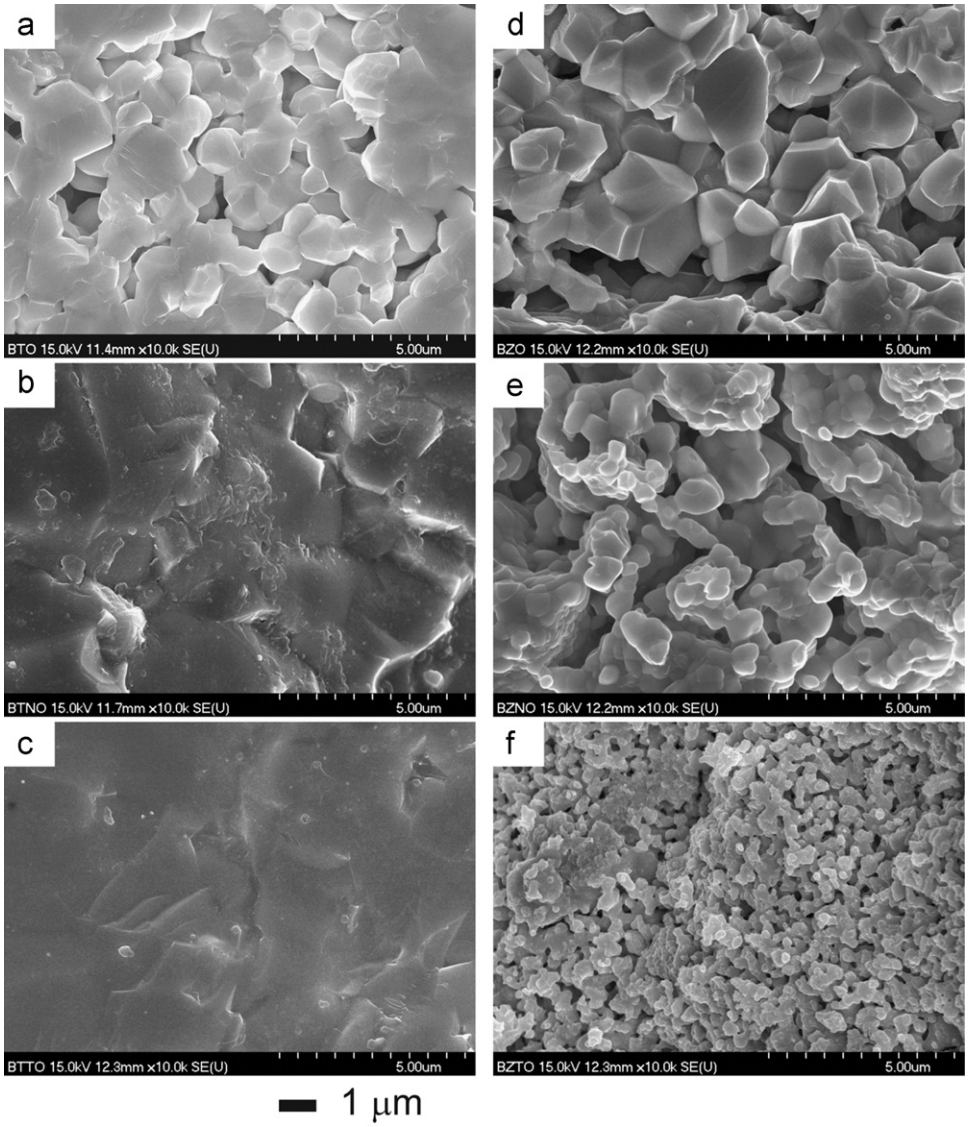

Fig. 2. SEM images of the fractured pellet surface of (a) BTO, (b) BTNO, (c) BTTO, (d) BZO, (e) BZNO, and (f) BZTO.

From BZO to BZTO, there was no symmetry transition but only slight lattice contraction. On the other hand, the diffraction peaks of BZTO were broadened remarkably compared to those of BZO. This suggests that the random distribution of Zr^{4+}, Ta^{5+} and vacancy (□) over the octahedral sites causes a decrease in the coherent crystallite size and an increase in micro-strain in the lattice, which is normal in solid solution systems [11]. Interestingly, BTNO and BTTO showed considerably less peak broadening, suggesting that they formed solid solutions with minimal disruption of lattice continuity.

Fig. 2 shows the microstructure of the sintered samples. The titanate samples tended to have a much larger particle size and higher density than the zirconate samples. The dopant effects on the microstructural evolution appear rather opposite in the two systems; Nb and Ta doping

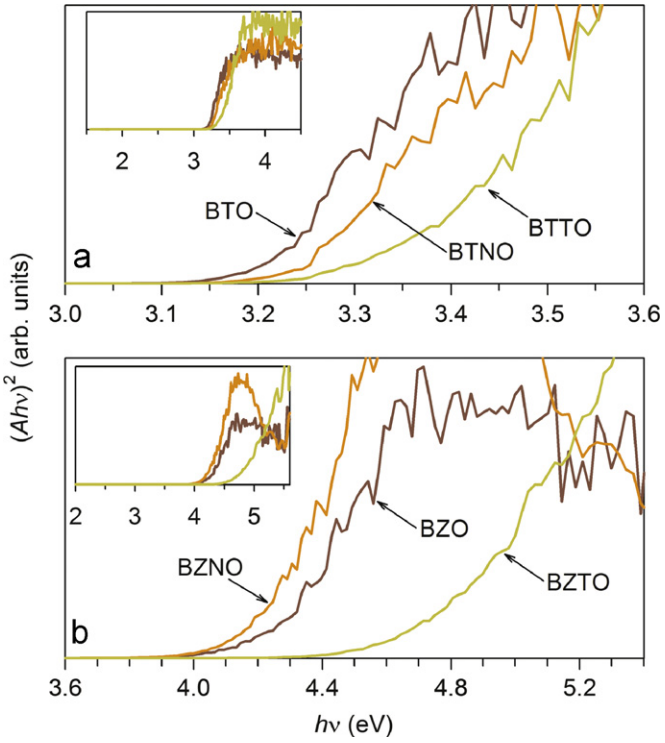

Fig. 3. Ultraviolet–visible absorbance spectra of (a) titanate and (b) zironate samples. The insets show the wide-range views.

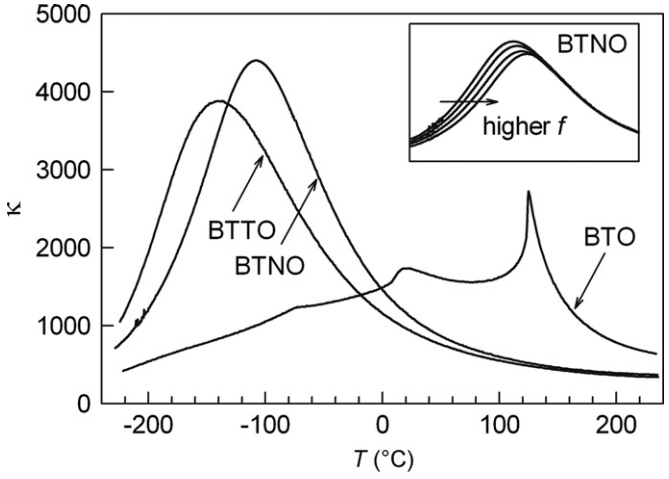

Fig. 4. Temperature-dependent κ of the titanate samples, at 100 kHz. The inset shows $\kappa(T)$ of BTNO measured at 1 kHz, 10 kHz, 100 kHz and 1 MHz.

increase the density and grain growth of BTO but decrease those of BZO.

The results suggest that the bonding characteristics of octahedral cations can affect solubility, crystallization and sintering. Because more electronegative cations are more prone to second-order Jahn–Teller distortion [12], they can tolerate better the local geometric distortions induced by the solid solution process. The facile crystallization of BTO, BTNO and BTTO can be attributed largely to Ti. The highly electropositive nature of Zr is responsible for the poor crystallization of BZTO and the failure to form a single phase of BZNO.

The absorbance spectra were recorded to determine the electronic structure of solid solution phases. As presented in Fig. 3, all samples exhibited inter-band transitions in the ultraviolet region. Although the BTO sample showed a direct gap transition with $E_g = 3.2$ eV, BTNO and BTTO had larger E_g values of 3.25 eV and 3.35 eV, respectively. Similarly, the E_g of BZTO (4.8 eV) was larger than that of BZO (4.25 eV). No indication of the reduced cation species (Ti^{3+}, Nb^{4+} and Ta^{4+}) was found. On the other hand, reduced oxides can be formed when heat-treated in a H_2 atmosphere [13].

Fig. 4 shows the temperature-dependent dielectric constants, $\kappa(T)$ of titanates, measured at 100 kHz. Upon cooling, BTO exhibited a paraelectric-to-ferroelectric phase transition near 125 °C, together with additional transitions at 17 °C and −72 °C, which correspond to sequential cubic-tetragonal–orthorhomic–rhombohedral transitions. BTNO and BTTO, however, showed only broad peaks of $\kappa(T)$, centered at −110 °C and −140 °C, respectively. For both cases, the temperature of κ_{max} was decreased gradually with the decreasing frequency, suggesting relaxor ferroelectric behavior. Detailed structural characterization in association with such a phase transition should be performed in future studies.

In the temperature range of the present investigation, the dielectric constants of the BZO-based solid solutions at room temperature were similar, 25.5, 24 and 26 for BZO, BZNO and BZTO, respectively. In all cases, the dielectric constants increased slightly with the decreasing temperature. When the porosity of the samples (≈ 0.2) is considered using the effective medium theory [14], the true dielectric constants can be estimated to be 35, 33 and 35.7, respectively, which is consistent with the reported value of BZO (38) [4]. Nb(Ta)-centered local dipoles may be quenched within the rigid zirconate lattice, resulting in an absence of polarization behavior.

4. Conclusions

Defect complex perovskites $(BaM_{0.9}M'_{0.1})_{0.984}O_3$ were formed for MM′ = TiNb (BTNO), TiTa (BTTO) and ZrTa (BZTO), with simple cubic average structures. BTNO and BTTO exhibited relaxor-like dielectric behavior arising from cation mixing on the octahedral sites. Diffuse maxima of $\kappa(T)$ were observed with $\kappa_{max} \approx 4500$, $T(\kappa_{max}) \approx -110$ °C for BTNO, and $\kappa_{max} \approx 3800$, $T(\kappa_{max}) \approx -140$ °C for BTTO.

Acknowledgments

This study was supported by the Yeungnam University Research Grant in 2011.

References

[1] A.S. Bhalla, R. Guo, R. Roy, The perovskite structure — a review of its role in ceramic science and technology, Materials Research Innovations 4 (2000) 3–26.

[2] L.G. Tejuca, J.L.G. Fierro, Properties and Applications of Perovskite-type Oxides, Marcel Dekker, New York, 1993.

[3] G.H. Kwei, A.C. Lawson, S.J.L. Billinge, S.-W. Cheong, Structures of the ferroelectric phases of barium titanate, Journal of Physical Chemistry 97 (1993) 2368–2377.

[4] S. Parida, S.K. Rout, L.S. Cavalcante, E. Sinha, M. SiuLi, V. Subramanian, N. Gupta, V.R. Gupta, J.A. Varela, E. Longo, Structural refinement, optical and microwave dielectric properties of $BaZrO_3$, Ceramics International 38 (2012) 2129–2138.

[5] T.A. Vanderah, R.S. Roth, T. Siegrist, W. Febo, J.M. Loezos, W. Wong-Ng, Subsolidus phase equilibria and crystal chemistry in the system BaO–TiO_2–Ta2O_5, Solid State Sciences 5 (2003) 149–164.

[6] R.D. Shannon, Revised effective ionic radii and systematic studies of interatomic distances in halides and chalcogenides, Acta Crystallographica A32 (1976) 751–767.

[7] A.C. Larson, R.B. Von Dreele, General Structure Analysis System, Los Alamos National Laboratory Report No. LAUR 86-748, Los Alamos, 2000.

[8] B.H. Toby, EXPGUI, a graphical user interface for GSAS, Journal of Applied Crystallography 34 (2001) 210–213.

[9] P. Kubelka, F. Munk, Ein beitrag zur optik der farbanstriche, Zeitschrift für Technische Physik (Leipzig) 12 (1931) 593–601.

[10] J.I. Pankove, Optical Processes in Semiconductors, Dover, New York, 1971.

[11] Y.-I. Kim, R. Seshadri, Optical properties of cation-substituted zinc oxide, Inorganic Chemistry 47 (2008) 8437–8443.

[12] I.B. Bersuker, Modern aspects of the Jahn–Teller effect theory and applications to molecular problems, Chemical Reviews 101 (2001) 1067–1114.

[13] K. Page, T. Kolodiazhnyi, T. Proffen, A.K. Cheetham, R. Seshadri, Local structural origins of the distinct electronic properties of Nb-substituted $SrTiO_3$ and $BaTiO_3$, Physical Review Letters 101 (2008) 205502/1–4.

[14] D.A.G. Bruggeman, Berechnung verschiedener physikalischer konstanten von heterogenen substanzen, Annalen der Physik (Leipzig) 24 (1935) 636–679.